Eur Biophys J (2008) 37:851–864
DOI 10.1007/s00249-008-0293-0

ORIGINAL PAPER

Insight into the recognition patterns of the ErbB receptor family transmembrane domains: heterodimerization models through molecular dynamics search

Oumarou Samna Soumana · Norbert Garnier · Monique Genest

Received: 8 November 2007 / Revised: 8 February 2008 / Accepted: 11 February 2008 / Published online: 26 March 2008

Abstract ErbB receptors undergo a complex interaction network defining hierarchical and competition relationships. Dimerization is driven entirely by receptor–receptor interactions and the transmembrane domains play a role in modulating the specificity and the selection of the partners during signal transduction. To shed light on the role of the GxxxG-like dimerization motifs in the formation of ErbB transmembrane heterodimers, we propose structural models resulting from conformational search method combined with molecular dynamics simulations. Left-handed structures of the transmembrane heterodimers are found preponderant over right-handed structures. All heterotypic heterodimers undergo two modes of association either via the N-terminal motif or the C-terminal motif. The transmembrane domain of ErbB3 impairs this C-terminal motif but also associates with the other partners owing to the presence of Gly residues. The two dimerization modes involve different orientations of the two helices. Thus, a molecular-switch model allowing the transition between the two dimerizing states may apply to the heterodimers and could help interpret receptor competition for the formation of homodimers and heterodimers. The comparison between experimental and theoretical results on the dimerization hierarchy of the transmembrane domains is not straightforward. However, we demonstrate that the intrinsic properties of the transmembrane sequences are an important component in heterodimer formation and that the ErbB2 and ErbB3 transmembrane domains have a strong power for heterodimerization as observed experimentally.

Keywords ErbB receptor family · TM domain · Heterodimerization · GxxxG motifs · Molecular dynamics · Computational search

O. Samna Soumana · N. Garnier · M. Genest (✉)
Centre de Biophysique Moléculaire, UPR 4301, CNRS,
University of Orléans, rue Charles Sadron,
45071 Orléans Cedex 02, France
e-mail: m.genest@cnrs-orleans.fr

O. Samna Soumana
e-mail: soumana@cnrs-orleans.fr

N. Garnier
e-mail: garnier@cnrs-orleans.fr

Introduction

The epidermal growth factor receptor (EGFR/ErbB1) belongs to a subclass of four receptors including ErbB2 in human (Neu in rodents), ErbB3 and ErbB4 (Ferguson et al. 2003; Yarden and Sliwkowski 2001). The ErbB receptors tyrosine kinase (RTKs) are involved in a wide range of differentiation and growth events and in the progression of carcinoma types (Citri and Yarden 2006; Salomon et al. 1995; Yarden and Sliwkowski 2001). ErbB receptors are transmembrane (TM) glycoproteins having three different domains: a variable extracellular ligand-binding domain at the N-terminal with two cysteine-rich sequences, a transmembrane spanning domain connected to the intracellular domain including a tyrosine kinase domain flanked by a large hydrophilic tail (Olayioye et al. 2000).

Ligand binding to the extracellular domain enhances the dimerization of the receptors or stabilizes existing, but unstable, dimers (Lemmon et al. 1997; Sako et al. 2000) and results in the cross-phosphorylation of the dimerized receptors (Olayioye et al. 2000; Schlessinger 2000). Pronounced differences in the mode of ligand binding have been revealed leading to homo-oligomers and hetero-oligomers in various combinations involved in signalization

across cell membrane (Linggi and Carpenter 2006; Warren and Landgraf 2006). All possible complexes between the receptors have been identified in different systems (Gullick 2001; Olayioye et al. 2000; Schlessinger 2000).

Relevant protein–protein interactions are beginning to be understood and significant insights into the molecular mechanisms of ErbB dimerization come from high-resolution structures of soluble ectodomains (Bouyain et al. 2005; Cho and Leahy 2002; Ferguson et al. 2003; Garrett et al. 2002, 2003; Ogiso et al. 2002). Ectodomain contacts between the two monomers occur, but their spatial proximity alone is not sufficient for receptor dimerization and efficient phosphorylation (Ferguson et al. 2003; Mattoon et al. 2004). Activation can be achieved without extracellular domains (Bargmann and Weinberg 1988a; Di Fiore et al. 1987) and dimers can form in the presence or absence of ligand (Moriki et al. 2001) suggesting that the basic ligand-induced dimerization mechanism is more complex than initially thought.

A series of findings indicate that regions other than the ectodomain contribute significantly to interactions. Contact regions exist between the kinase domains and involve two lobes termed N and C lobes (Zhang et al. 2006). The cyto-juxtamembrane region of each ErbB receptor contains basic residues that influence dimerization (Aifa et al. 2005, 2006). Dimerization involves also direct contacts between the helical TM segments of the receptors (Fleishman et al. 2002; Li and Hristova 2006; Mendrola et al. 2002).

The potential implication of the TM domain is illustrated by the Neu mutation in the ErbB2 that provokes constitutive dimerization and kinase activation (Bargmann et al. 1986; Bargmann and Weinberg 1988a, b). The close association between these domains is presumed to be driven by the GxxxG dimerization motif (x is any residue) originally described by Sternberg and Gullick (1990). In this motif, Gly can be replaced by a small residue (Ala, Ser or Thr; Dawson et al. 2002, 2003; Eilers et al. 2002; Kleiger et al. 2002; Senes et al. 2000).

All ErbB receptors have a single TM domain that exhibits a conserved and very common GxxxG-like motif at both the N-terminal and the C-terminal ends, except ErbB3 for which this motif is present only at the N-terminus. The presence of this motif correlates with the degree of self-association of the ErbB TM spans (Mendrola et al. 2002). It is also suggested that the Neu mutation (V659E) when introduced into ErbB2 induces a shift between two packing modes, which may represent active and inactive configurations of the receptor (Fleishman et al. 2002). These two motifs in the ErbB1-ErbB2 heterodimer could exert a separate function in TM domain assembly, one for homodimerization and the other for heterodimerization (Gerber et al. 2004). The ErbB TM segments isolated from the full-length protein are not independent association domains in micellar environment, but helix–helix interactions exist and require stabilizing interactions by other parts of the receptor (Stanley and Fleming 2005). The association of the receptors comes from the sum of many interactions including weak contacts distributed throughout all the domains. In addition, ligand binding also induces a rearrangement of each receptor subunit owing to the rotation of the TM domains (Bell et al. 2000; Moriki et al. 2001).

Receptor–receptor interactions display distinct selectivity that defines hierarchical and competitive relationships (Karunagaran et al. 1996; Prigent and Gullick 1994). Biochemical experiments undertaken on the four human ErbB receptors (Tzahar et al. 1997) revealed that from the six possible heterotypic interactions within the family, three are involved in relatively strong inter receptor interactions. ErbB2 acts as the preferential partner of the ligand-bound ErbB1, ErbB3 and ErbB4, and its major partner is the kinase-defective member of the family ErbB3. Heterodimers between ErbB3 and ErbB4 are not detectable. These results agree on many aspects with the study undertaken by Riese et al. (1995).

Recent experimental studies using FRET (fluorescence resonance energy transfer) (Duneau et al. 2007) have shown that the association of the TM domains of the four ErbB receptors obeys a hierarchy very similar to that observed for the whole receptors. FRET studies revealed that the TM domain of ErbB2 is the preferential partner of the other receptors with a marked preference for that of ErbB3 and ErbB1, while the association of the TM domains of ErbB4 and ErbB2 is found to be less favorable. Other heterodimers involving the ErbB1 TM span are observed and ErbB3-ErbB4 TM species are detected. Thus, the TM domain of the ErbB receptors is presented as a selector of the population of dimer species, which plays a major role in modulating the affinity, specificity and the selection of partners during signal transduction.

Although the TM domain does not provide a unique driving force to stabilize the receptor dimers, it seems important to shed light on how the TM domains associate in the context of heterodimer formation. The details of the interactions between the TM domains and the knowledge of their structure could help in understanding the role of the juxtamembrane segment at the junction of the TM domain and the N-lobe of the kinase domain, which is believed to maintain a certain flexibility allowing switch positions to activate each receptor.

Transmembrane domain association is governed both by the intrinsic properties of the peptide sequence and by peptide–lipid interactions. The present study only focuses on the intrinsic properties of the peptide sequences. To address this question, the six possible heterotypic interactions have been studied. To identify possible structures of

the heterodimers, a global search method combined with molecular dynamics (MD) simulations starting from 1,296 initial structures for each type of interactions is used. The protocol, recently described (Samna Soumana et al. 2007), successfully predicts the right-handed structure of the TM dimer of glycophorin A (MacKenzie et al. 1997). When applied to the TM association of ErbB2-ErbB3, it was shown that the best structures conform to the presence of the GxxxG-like dimerization motifs at the dimer interface.

The present results show a net preference for a left-handed structure of TM helix pairs over a right-handed structure for all the heterodimers. The most representative MD models exhibit the presence of either one of the two dimerization motifs at the contacting interface. The two dimerization modes presumed to be involved in the complex interaction network of the receptors are discussed in relation to experimental data. Interaction hierarchy is compared to experiments on the whole receptors and the TM domains (Duneau et al. 2007; Tzahar et al. 1996).

Methods

TM domain systems

The six helical heterodimers within the ErbB receptor family are studied. For clarity, the TM domain and the whole receptor will be noted as HER_{TM} and ErbB, respectively. Thus, the transmembrane heterodimers will be named $HER^{i-j}{}_{TM}$ ($i = 1$–4, $j > i$). Each monomer includes 25 residues of the TM hydrophobic sequence of each receptor (ErbB1 (Ullrich et al. 1984), ErbB2 (Coussens et al. 1985; Yamamoto et al. 1986), ErbB3 (Kraus et al. 1989), ErbB4 (Plowman et al. 1993)). The sequences are given in Table 1. Each heterodimer comprises two helices, each built with the amino terminus acetylated and the carboxyl terminus methyl-aminated to mimic the peptide bond.

Table 1 Sequences of the TM domain of the four ErbB receptors: $HER^1{}_{TM}$ (Ullrich et al. 1984), $HER^2{}_{TM}$ (Coussens et al. 1985; Yamamoto et al. 1986), $HER^3{}_{TM}$ (Kraus et al. 1989) and $HER^4{}_{TM}$ (Plowman et al. 1993)

TM domain	Sequence	Residues
HER1	PSIA**TGMVG**ALLLLLVVALGIGLFM	644–668
HER2	LT**SIVSA**VVGILLVVVLGVVFGILI	651–675
HER3	LTMALTVIAGLVVIFMMLGGTFLYW	642–666
HER4	PLIAAGVIGGLFILVIVGLTFAVYV	651–675

The regions corresponding to the putative GxxxG dimerization motif in each TM domain are shaded gray. SmxxxSm interactions sites are in bold or underlined (see text)

Computational search

The program CHARMM Version 26 (Brooks 1983) and the all hydrogen PARAM22 force field (MacKerell et al. 1998) were used in the present study. All calculations were carried out in vaccum and performed on a multi-processor platform Linux Beowulf cluster with dual 3.06 GHz Intel Xeon processors.

Conformational sampling and MD protocol have been detailed in a previous paper (Samna Soumana et al. 2007). The main steps of the MD search are summarized in the following text and illustrated in Fig. 1.

Initial structures

Parallel dimers were first generated with two helices (H1 and H2) built with the standard torsion angles. For a complete search over the two-body rotational interaction space, helices were rotated about their own axis by 10°

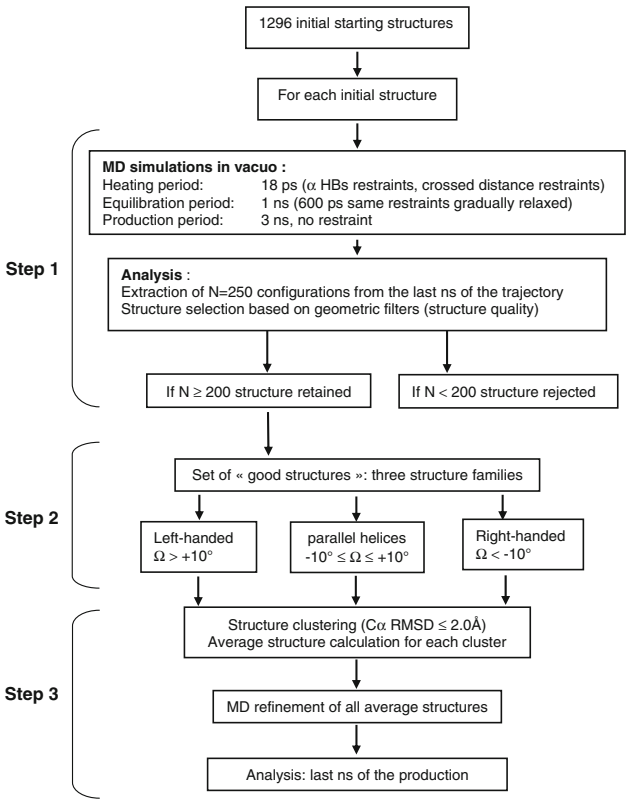

Fig. 1 Flowchart giving an overview of the main steps of the search protocol and MD simulations applied to the prediction of heterodimerization of the TM domain of the ErbB receptor family. Details of the method are given in our previous work (Samna Soumana et al. 2007)

steps for a complete rotation. A total of 1,296 (36 × 36) initial structures were generated for each heterodimer. For each initial structure, the two helices were separated by a distance Dh between the helix axes corresponding to the minimum distance to prevent steric contacts (Samna Soumana et al. 2007). This is obtained by combining energy minimization and the progressive approach of the two helices maintained in a parallel orientation.

MD simulations

All the 1,296 initial structures were submitted to MD simulations at constant temperature ($T = 300$ K). Thermalization was performed by increments of 50 K by maintaining the two helices close to the α structure, while restricting a vertical shift of one helix relatively to the second helix. Backbone hydrogen bonds (α H bonds) and crossed distances restraints (see Table 2 for definition) were applied and the force constant was gradually reduced in the course of the equilibration period. The production period was continued for 3 ns without any restraint. Atomic coordinates and energy terms were saved every picosecond (ps). The last nanosecond (ns) of the trajectories served for averaging and analyses.

Analysis

The analysis of the dimers consists in the selection of the best structures based only on geometric criteria and not on energy criteria. A structure is considered to be correct when its geometry is compatible to that of a TM dimer embedded within a lipid bilayer. Three steps are applied to control the quality of a dimer structure.

Step (1): Six geometric conditions (Table 2) are imposed to each of the 250 configurations extracted from the last ns MD trajectory (one configuration extracted every 4 ps). Helix distortions and helix register (ΔZ) that defines the vertical shift of the helices relatively to each other are accepted, but limited (Killian and von Heijne 2000; Weiss et al. 2003). The two helices must exhibit a similar degree of helicity and this feature is controlled by the difference between the crossed distances (Δ_{dc}). These three criteria give an account of a suitable complementarity of the facing side chains at the dimer interface. The crossing angle between the two helices must be between −65° and 45°, as observed in membrane proteins (Bowie 1997).

A configuration is structurally correct when all the six parameters are respected, otherwise the configuration is rejected. A structure of the dimer is accepted when 200 configurations are structurally correct (80%). This value corresponds to the standard deviation of a hypothetic normal distribution.

Step (2): The retained structures are grouped in three families depending on the crossing angle value that defines right-handed coiled-coil, left-handed coiled-coil or dimers with parallel helices.

Step (3): In each family, similar structures are clustered (Cα RMSD ≤ 2 Å) to reduce the number of dimer structures. For each cluster, an average structure is calculated and energy minimized and the same exact MD protocol as described previously is applied for further refinement. Then, geometric filters are applied for the control of the quality of the refined structure.

Particular attention was given to the choice of the criteria and their strength in order to obtain a reasonable number of final structures. The criterion that is most sensitive is the difference between the crossed distances (Δ_{dc}) (55% of the configurations are eliminated in average against 30% for the control of helix length and the vertical shift of the helices). The crossing angle value is less selective (7% of the configurations are eliminated in average). We have also verified that the criteria are not correlated. Two or three criteria can exclude the same configurations, but the number of configurations eliminated is different. Structure exclusion only depends on the orientation of the helices.

Furthermore, a threshold of 80% of configurations imposed to decide if a structure was correct was tested. A value of 70% leads to a larger number of correct

Table 2 Parameters defining the dimer structure quality (Samna Soumana et al. 2007)

Parameters	$L_{H\alpha}$ (Å)		Δ_{dc} (Å)	$\Delta Z_{Nter}\Delta Z_{Cter}$ (Å)	Ω (°)	
	Minimum	Maximum			Minimum	Maximum
HER_{TM}	32.0	38.0	≤3.5	≤3.5	−65°	+45°

L_H is the length of an α canonical helix ($L_{H\alpha} = 35.25$Å for a 25 residue helix). $L_{H\alpha}$ is the distance between the C_α atoms of the first residue C_α^HNter and the last residue C_α^HCter. Δ_{dc} is the difference between the crossed distances (C_α^{H1}Nter − C_α^{H2}Cter and C_α^{H2}Nter − C_α^{H1}Cter). Crossed distance: distance between the C_α atoms of the first residue C_α^HNter of one helix (H1 or H2) and the C_α atoms of the last residue C_α^HCter of the second helix (H2 or H1). ΔZ(Nter) = [($Z(C_\alpha^{H1}$ Nter) − $Z(C_\alpha^{H2}$ Nter)] is the difference in Z positions of the C_α atoms of the first residue of H1 and H2. Same definition for ΔZ(Cter) but for the C_α atoms of the last residue of H1 and H2. Ω (°) is the crossing angle calculated following the method of Chothia et al. (1981) included in CHARMM. Crossing angle values (minimum, maximum) are from Bowie (1997) and deduced from statistical analysis of membrane proteins

configurations, particularly for the left-handed structures, which are found to be preponderant. After clustering and structure averaging, approximately the same number of clusters is obtained and consequently the same number of final refined structure.

Helix–helix interactions are calculated for the final MD dimer models. To distinguish between the structures, an appropriate term is the gas-phase contribution to the binding free energy $\Delta G°_{bind}$ (Zoete et al. 2005). This term includes the conformational cost for the dimerization and the interaction energy term between the two helices. We keep in mind that this term does not represent correctly the free energy of association of the helices. Helix–helix affinity can be modulated by the membrane environment and this point will be discussed below.

$\Delta G°_{bind}$ is calculated as: $\Delta G°_{bind} = \Delta E_{intra} + E_{vdW} + E_{elec}$ where ΔE_{intra} is the difference between the sum of the internal energies of the two helices in the dimer ($E^{D}{}_{intra}$) and the sum of the internal energies of the two isolated helices ($E^{H1}{}_{intra} + E^{H2}{}_{intra}$). E_{vdW} and E_{elec} are the van der Waals and electrostatic interaction energies calculated between the two helices. Contacting surface areas were also evaluated (Samna Soumana et al. 2007).

Results

Global analysis of the $HER^{i-j}{}_{TM}$ models

From the 1,296 sampled structures for each heterodimer type, three families representative of the right-handed, left-handed and parallel dimers were obtained. The number of the selected structures for the different families given in Table 3 clearly shows a net preference for dimers with helices in left-handed interactions. Very few right-handed structures result from geometric filtering except for the two heterodimers $HER^{2-1}{}_{TM}$ and $HER^{2-4}{}_{TM}$. Dimers with parallel helices (absolute value of the crossing angle less than 10°) are well represented for the association of $HER^{4}{}_{TM}$ with $HER^{2}{}_{TM}$ or $HER^{3}{}_{TM}$. These structures, named "good" structures, represent a percentage ranging from 5 to 13% of the 1,296 initial structures.

The distribution of the crossing angles (Fig. 2) shows helix–helix angles centered around 25°–35° for the left-handed structures. For the structures defining right-handed coiled coils, the crossing angle ranges between −30° and −10°. The two peaks around ±5° correspond to the large population of the dimers with parallel helices found for the heterodimers $HER^{2-4}{}_{TM}$ and $HER^{3-4}{}_{TM}$.

The magnitude of helix–helix interactions is an indicator of the affinity of the two partners. van der Waals interactions are dominant and represent 70% or more of the total interactions calculated between the two helices. Electrostatic interactions are negative and greatly vary depending on the nature of the residues at the interface.

Helix–helix interactions range in average between −75 and −43 kcal/mol for most of the $HER^{i-j}{}_{TM}$ heterodimer models. The strongest interactions between the two helices come from the electrostatic term owing to the presence of a Thr side chain facing a small residue at the interface. The very short Cα–Cα distance (3.9 Å) between Thr643 and Gly656 in one $HER^{3-4}{}_{TM}$ model leads to helix–helix interactions of −84 kcal/mol in average.

Another parameter that may help in evaluating the affinity of the two monomers is the binding free energy $\Delta G°_{bind}$. If we consider all MD selected models (data not shown) obtained after the final selection (step 3), $HER^{2-3}{}_{TM}$, $HER^{1-3}{}_{TM}$ and $HER^{3-4}{}_{TM}$ exhibit the best affinity compared to the three others.

Contacting surface area between the two helices informs on the way the two helices interact. For the whole set of correct structures defined for the six types of heterodimers, the contacting surface area varies from 640 $Å^2$ ($HER^{2-4}{}_{TM}$ and $HER^{1-4}{}_{TM}$) to 685 $Å^2$ ($HER^{3-4}{}_{TM}$ and $HER^{1-3}{}_{TM}$). Models of $HER^{2-1}{}_{TM}$ and $HER^{2-3}{}_{TM}$ exhibit, in average, a contacting surface of 655 and 669 $Å^2$, respectively.

Table 3 Summary of the simulations

HER_{TM} heterodimer	Structure family	HER^{2-1}	HER^{2-3}	HER^{2-4}	HER^{3-4}	HER^{1-3}	HER^{1-4}
Nb of selected structures after step 1	L	91	77	73	60	86	58
	P	22	20	69	54	3	8
	R	14	2	31	2	1	2
Percentage of "good" structures after step 1		10	8	13	9	7	5
Nb of selected structures after step 3	L	11	5	5	9	9	5
	P	2	1	3	1	0	0
	R	1	1	0	1	1	1

Selected structures for the different HER_{TM} heterodimers after geometric filters (step1) and after structure clustering and final MD refinement (step 3). Three families of dimer models are found: left-handed coiled coil (L); right-handed coiled coil (R) and dimers with parallel helices (P). Percentage of "good" structures is calculated over the 1,296 initial configurations simulated for each heterodimer

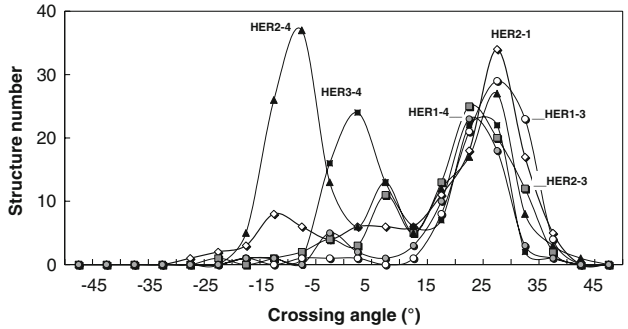

Fig. 2 Distribution of the crossing angles Ω (°) calculated for the HER_{TM} heterodimers models resulting from geometric filters. Left-handed structures are dominant with Ω ranging between 20° and 35°. $HER^{2-4}{}_{TM}$ and $HER^{3-4}{}_{TM}$ heterodimers are characterized by a large number of parallel dimers $\Omega = \pm 5°$. Very few right-handed structures are formed between the TM domains

GxxxG-like motifs mediate HER_{TM} association

The predominance of small residues at helix–helix interface is recognized as a main property of helices in membrane proteins (Adamian and Liang 2001; Eilers et al. 2000; Gratkowski et al. 2001; Javadpour et al. 1999; Walters and DeGrado 2006; Zhou et al. 2001). SmxxxSm motifs (Sm is a small residue Gly, Ala, Ser or Thr and x is any residue) are present in all ErbB TM domains. Search for residues in short contacts (Cα–Cα distance between the TM monomers ≤6 Å) have been undertaken on the whole final MD models. The results are shown in Fig. 3. The plots clearly evidence that the residues of the motifs appear at the dimer interface with a high occurrence. In the case of $HER^{1}{}_{TM}$, Ser645, Ala647, Thr648, Gly649 at the N-terminus and Ala661 and Gly665 at the C-terminus are the most frequent. For $HER^{2}{}_{TM}$, all the small residues, particularly the polar residues Ser and Thr at the N-terminus and the Gly residues of the C-terminus are also the most frequent. The same observation is made for $HER^{4}{}_{TM}$ with a strong implication of Gly and Ala and for $HER^{3}{}_{TM}$ with a predominance of the polar residues Thr643 and Thr647 of the N-terminal motifs oriented inside the interface. Despite the fact that $HER^{3}{}_{TM}$ is the only domain without putative dimerization motif at the C-terminal side, the two Gly residues 660–661, at a similar position to that of the second dimerization motif of the other HER_{TM} domains, frequently occur in close proximity with the facing helices.

From this analysis, we demonstrate that small residues of the SmxxxSm motifs of the ErbB TM domains are predominant at the dimer interface. This result is in total accordance with the role of these motifs in helix–helix association in membrane proteins and particularly in ErbB receptor dimerization. MD models can be regarded as representative models of HER TM domain association.

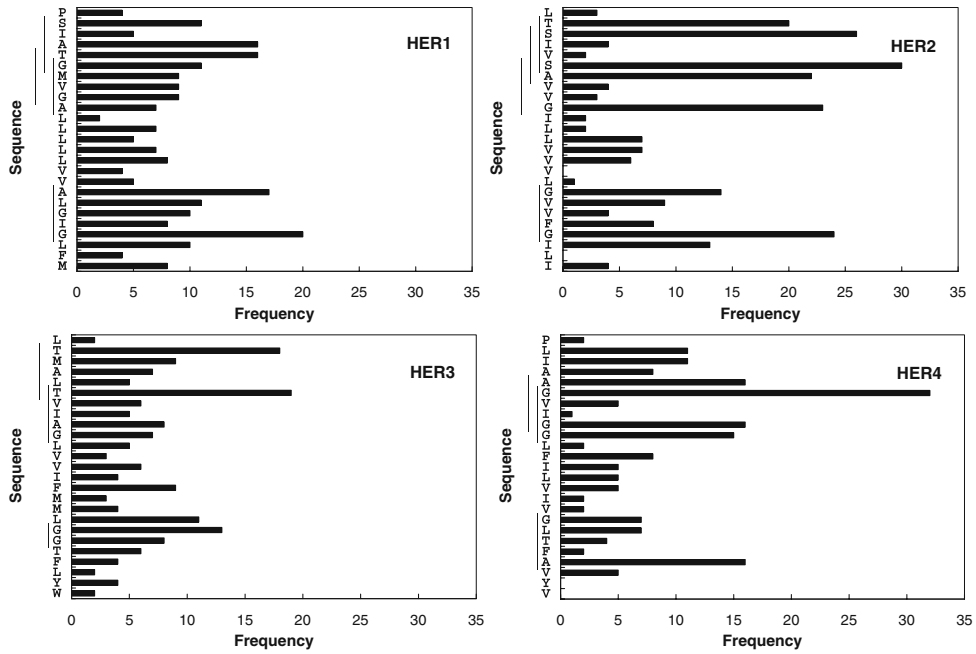

Fig. 3 Statistics on inter helix–helix distances. Number of times the residue R_k of the monomer $HER^{i}{}_{TM}$ ($i = 1 - 4$) is close to any residue R_l of the second monomer $HER^{j}{}_{TM}$ ($j = 1 - 4$, $j \neq$ i): distance $C_\alpha R_k - C_\alpha R_l \leq 6$ Å. The analyses use the structures of all the heterodimers $HER^{i-j}{}_{TM}$ (six types) resulting from the final selection (see Table 1). The number of residue pairs examined is 223 for HER^{1}, 238 for HER^{2}, 170 for HER^{3} and 187 for HER^{4}. The GxxxG-like motif of the HER_{TM} sequences and the extended motifs SmxxxSm are underlined. $HER^{3}{}_{TM}$ exhibits only one GxxxG motif at the N-terminal side. The two Gly residues at a position similar to that of the C-terminal motif found in all others sequences are highlighted

Table 4 Characteristics of the $HER^{i-j}{}_{TM}$ heterodimers models

	HER^{i-j} TM	Motif	Ω	D_{Hi-Hj}	$D_{C\alpha i-C\alpha j}$	$R_{Hi} - R_{Hj}$	SA	E_{inter}	$\Delta G°_{bind}$	E_{inter} Motif	
										N ter	C ter
$HER^{2}{}_{TM}$ partners	HER^{2-1}	N ter	−12	8.4	4.3	G660-G652	632	−66	−152	−5	−2
		N ter	0	8.6	4.2	T652-S645	741	−76	−151	−1.2	−3
		C ter	22	8.1	4.7	G672-F667	721	−69	−144	−1	−2
	*HER^{2-4}	N ter	40	6.8	4.1	A657-G659	627	−57	−149	−0.8	−7.4
		C-ter	−10	5.5	4.7	V665-V665	595	−43	−136	−0.7	−2.6
	HER^{2-3}	N ter	24	8.1	4.4	A657-T647	687	−65	−161	−4.1	−4.1
		C ter	13	8.7	4.8	G668-G660	590	−42	−140	−1.7	−1.7
$HER^{3}{}_{TM}$ partners	HER^{1-3}	N ter	23	8.1	4.7	M650-T647	709	−69	−185	−7.1	−7.1
		C ter	21	8.2	4.8	L666-G661	672	−62	−178	−3.8	−3.8
	*HER^{3-4}	N ter	27	7.8	4.8	T647-G656	734	−72	−180	−4.6	−4.6
		C ter	23	8.2	4.3	G660-G668	673	−45	−139	−1.4	−1.4
$HER^{4}{}_{TM}$ partners*	*HER^{1-4}	N ter	21	9.1	5.3	A647-A655	641	−46	−141	−1.5	−1.9
		C ter	28	7.8	4.2	G665-A672	603	−42	−129	−2.5	−4.9

All the selected structures are not detailed. Two examples of association via the N-terminal motif and the C-terminal motif are given for the different heterodimers (see text). Right-handed structures are characterized by a negative value of the crossing angle (Ω) and left-handed structures are characterized by a positive value. Helix–helix angle is between −10° and +10° for parallel dimers. Crossing angle Ω (°) is calculated following a method by Chothia et al. (1981) included in CHARMM. $E_{inter\ motif}$ is calculated between the GxxxG dimerization motif at the N-terminus and the C-terminus. Energy terms are in kcal/mol

D_{Hi-Hj} (Å): inter-helical distance between the two helices; $D_{C\alpha i-C\alpha j}$ (Å): minimum distance between Cα atoms of opposed residues $R_{Hi} - R_{Hj}$. SA (Å^2): contacting surface area at the dimer interface. E_{inter}: helix–helix interactions. $\Delta G°_{bind}$: mean value of the gas-phase contribution to the binding free energy (see text for definition)

* Heterodimers formed with $HER^{4}{}_{TM}$

Structures and characteristics of the heterodimers

All the $HER^{i-j}{}_{TM}$ models will not be detailed in the following. Only the models for which either the N-terminal motif or the C-terminal motif is well positioned at the dimer interface are discussed in the following text. Energetic and geometrical characteristics are given in Table 4.

$HER^{2}{}_{TM}$ and its partners

Among the 14 "good" structures retained for the $HER^{2-1}{}_{TM}$ heterodimers, three structures are presented. One is a right-handed structure with the two helices crossed with a small angle. This structure exhibits helix–helix interactions mediated by the N-terminal motif. The shortest residue–residue distance is observed between the two facing Gly residues 660 and 652 of $HER^{1}{}_{TM}$ and $HER^{2}{}_{TM}$, respectively. It is the only structure, which exhibits a strong inter helical HB between the carbonyl group of Thr648 on $HER^{1}{}_{TM}$ and the side chain of Ser656 on $HER^{2}{}_{TM}$. The second structure representative of the $HER^{1}{}_{TM}$ and $HER^{2}{}_{TM}$ association exhibits parallel helices in tight contacts all along the interface explaining a large contacting surface. The polar residues Ser645 and Thr648 of $HER^{1}{}_{TM}$ and Thr652 and Ser656 of $HER^{2}{}_{TM}$ pertaining to the SmxxxSm motifs are in close proximity. Gly residues of the C-terminal motifs are buried within the dimer interface. For this model, the contribution of this last motif to helix–helix association is slightly stronger than that calculated for the N-terminal motifs. The Phe residues, with their bulky side chain oriented within the dimer interface, contribute to an increase of inter helical van der Waals interactions.

The left-handed structures constitute the main family of the $HER^{2-1}{}_{TM}$ heterodimers. One structure with helices crossed at 22° represents this family. The magnitude of helix–helix interactions is very comparable to the previous ones. The shortest residue–residue distances are observed at the C-terminal extremity at the level of the two terminal motifs. In average, the two motifs contribute weakly to the helix–helix interactions. For these $HER^{2-1}{}_{TM}$ MD models, the GxxxG-like motif, either at the N-terminus or at the C-terminus exerts favorable, but weak, intermolecular interactions. Energy values are generally not lower than −5 kcal/mol. Motif–motif interactions result from the sum of van der Waals interactions, which are dominant, and weak electrostatic interactions. A weak contribution of the GxxxG dimerization motifs to helix–helix interactions appears to be a common characteristic of all MD models.

Very few "good" structures are obtained for the HER^{2}-HER^{3} TM association. Some of the models have been presented in our previous paper. Here, only two of them (referred to as L1 and L4 in Samna Soumana et al. (2007))

are recalled. The N-terminal motif appears to be the mediator of interhelical interactions, but it is observed that tight helix–helix contacts can be formed at the C-terminal side. This result was not expected owing to the absence of dimerization motif at this extremity for $HER^3{}_{TM}$. As it will be shown below, the heterodimers formed with $HER^3{}_{TM}$ are characterized by the presence of Gly660 or Gly661 at the dimer interface. One of the two models presented in Table 4 is the most stable of the $HER^{2-3}{}_{TM}$ ensemble. The two residues of the N-terminal motif, Ala657 and Thr647, respectively, on $HER^2{}_{TM}$ and $HER^3{}_{TM}$, are in a close approach giving rise to strong helix–helix interactions. The second model is also a left-handed structure, slightly less stable than the former with short Gly–Gly interhelical distances at the C-terminus. Helix–helix interactions are much less favorable than for the previous structure. Figure 4 represents these two structures and highlights the dimer interface. Interestingly, each of the two modes of association corresponds to a particular orientation of the two helices. This result will be discussed in the following.

$HER^4{}_{TM}$ appears as a very bad partner of $HER^2{}_{TM}$. Interhelical interactions are slightly less favorable than those calculated for the other types of heterodimers. $HER^4{}_{TM}$ is the only TM span without polar residues at the N-terminus leading to weak electrostatic interactions between the helices. For this type of heterodimer, helix–helix association is essentially governed by the van der Waals interactions. It is to be noted that for most of the final $HER^{2-4}{}_{TM}$ models, the structure of the two monomers was often found to be far from the regular α helix (limit of the geometric criteria). Helix distortions are probably induced by the presence of bulky side chains (Phe, Tyr), which are aligned along the same helix face composed of small residues. Two different structures representative of the HER^2–HER^4 TM association are detailed. One is a left-handed structure with a large crossing angle (40°) and a very short distance at the crossing point. The second structure shows two helices nearly parallel in weak interactions where Gly668 and Gly672 on $HER^2{}_{TM}$ and Gly668 on $HER^4{}_{TM}$ favor tight contacts at the C-terminal side. For this association, the bulky Phe and Tyr side chains are oriented outside the interface and electrostatic interactions are null. For this model, helix–helix separation is short compared to the other types of heterodimers.

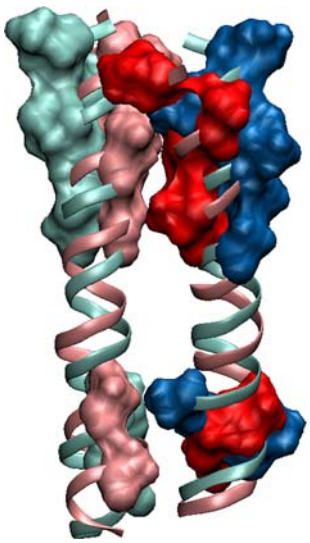

Fig. 4 $HER^{2-3}{}_{TM}$ heterodimer. The two structures described in Table 4 are superimposed (Cα atoms of the backbone). Small residues including Gly, Ala, Ser and Thr are represented by their vdW surface. The association mediated by the N-terminal motif shows the contacting surface between the residues of $HER^2{}_{TM}$ (*pink*) and the residues of $HER^3{}_{TM}$ (*red*). For this association, the Gly residues of the C-terminal motif of $HER^2{}_{TM}$ and at the C-terminal side of $HER^3{}_{TM}$ are out of the interface. When helices associate via the C terminus, the Gly residues are oriented within the interface ($HER^2{}_{TM}$: *light blue*, $HER^3{}_{TM}$: *blue*) and the small residues of the N-terminus are out of the interface

$HER^3{}_{TM}$ and its partners

The TM domain of the ErbB3 receptor associates favorably with the other TM domains of the family. The most representative structures of the association with $HER^3{}_{TM}$ are left-handed coiled coils. When helix–helix association is mediated by the N-terminal motif, Thr647 is the most frequently involved at the dimer interface. At the C-terminal side, Gly660 or Gly661 are often observed at the dimer interface. This is shown in Fig. 5. These two Gly residues are followed by a Thr residue, which participates to low HB's interactions with residues of the facing helix. For the three types of heterodimers including $HER^3{}_{TM}$, helix–helix interactions are generally the strongest when the N-terminal motif residues are in a close approach. In the case of HER^1–HER^3 TM association, electrostatic interactions can be relatively strong compared to the van der Waals interactions (ratio 1:2). This same observation is made for $HER^{2-3}{}_{TM}$ and $HER^{3-4}{}_{TM}$ heterodimers owing to the presence of residue Thr647 at the interface. Short Cα–Cα distances are observed between 4.3 and 4.8 Å and characterize the proximity of the small residue motif at the dimer interface. The other heterodimer models formed with $HER^3{}_{TM}$ exhibit Cα–Cα distances greater than 5.5 Å depending on the nature of the residue pairs at the dimer interface (data not shown).

$HER^4{}_{TM}$ and its partners

The behavior of two partners of $HER^4{}_{TM}$ has been described previously showing that the association with $HER^3{}_{TM}$ can be more favorable than with $HER^2{}_{TM}$. The association with $HER^1{}_{TM}$ appears to be less favorable. The two structures described in Table 4 are left-handed coiled

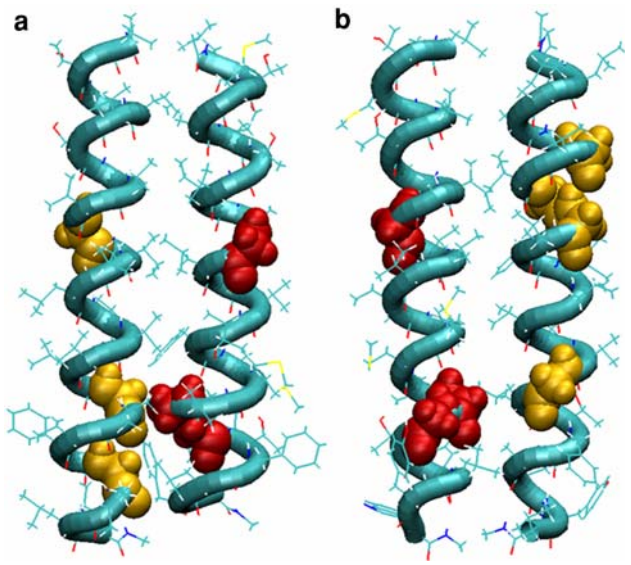

Fig. 5 Gly residues at the dimer interface of the heterodimers formed with $HER^{3}{}_{TM}$. **a** $HER^{2-3}{}_{TM}$ heterodimer. **b** $HER^{3-4}{}_{TM}$ heterodimer. The Gly residues are represented by van der Waals surfaces. Gly on $HER^{3}{}_{TM}$ are in *red*, Gly on $HER^{2}{}_{TM}$ and $HER^{4}{}_{TM}$ are colored *yellow*. Views of the helices from the N-terminus (*top*)

coils with almost regular helices. Helices are not vertically shifted and in both models the small Ala and Gly residues of either the N-terminal motif or the C-terminal motif are in contact at the interface. As noted before, the particularity of the TM domain HER^{4} is the absence of polar residues at the N-terminal side that may explain weak helix–helix interactions at the level of the dimerization motif.

All the heterodimer models have their helices at a distance of around 8.2 Å in average, which is slightly shorter than that observed for left-handed coiled coils in membrane proteins. Very negative values calculated for the binding free energy are correlated to strong helix–helix interactions. Larger the contacting surface, more stable is the dimer due to strong van der Waals interactions. Such a correlation between strong helix–helix interactions and large contacting surface area is well evidenced for the left-handed structures. Obviously, the magnitude of the contacting surface area depends on the orientation of the two helices relative to each other.

Discussion

Receptor–receptor interactions in the ErbB family display distinct selectivity defining hierarchy and competition relationships (Prigent and Lemoine 1992; Riese et al. 1995; Tzahar et al. 1996). Until recently, activation of the ErbB receptors was attributed to ligand-induced dimerization of the extracellular domains of the receptor, but numerous data tend to demonstrate that receptors can associate prior to ligand binding. Other dimerization sites, distinct from extracellular sites, can mediate homo and heterodimerization. Specifically, the two GxxxG consensus motifs in the TM span that are able to induce intrinsic dimerization (Mendrola et al. 2002) may explain the hierarchy, the competition and directionality of receptor–receptor contacts. The power of heterodimerization of the TM spans has been recently studied by fluorescence resonance energy transfer (FRET; Duneau et al. 2007) showing the ability of the TM helix pairs to form dimers varying from non-interactive pairs to strong dimerization. $HER^{2}{}_{TM}$ appears to be the TM span having the largest tendency to heterodimerize with $HER^{3}{}_{TM}$ and $HER^{1}{}_{TM}$.

In this paper, we proposed structural models of all heterotypic heterodimers from exhaustive conformational search and MD simulations. Models are designed only on the basis of peptide sequences and reflect only their intrinsic properties. Environmental effects are omitted.

The recognition motifs

The main finding of this study is that the SmxxxSm motifs are recognition patterns of the TM domain of the ErbB family. For all the heterodimers, TM helix pairs form stable structures when the small residues, namely Gly, Ala, Ser and Thr are dominant at the dimer interface. This result conforms to helix–helix packing observed in membrane proteins (Adamian and Liang 2001; Javadpour et al. 1999). Our MD models describe two dimerization modes for all the TM heterodimers including the heterodimers formed with $HER^{3}{}_{TM}$ that impairs the second C-terminal motif. TM domain association via the N-terminus generally leads to the strongest helix–helix interactions and binding free energy values. In the case of $HER^{1-3}{}_{TM}$, interactions are almost equivalent for the two modes of association.

Experimental studies suggest that these two motifs have a different role in the dimerization process. The TM domains of the ErbB receptors self-associate strongly in the absence of the extracellular domain (Mendrola et al. 2002) and it was suggested that in the case of ErbB2/Neu one of the two motifs would promote the formation of an active conformation. Computational studies on the ErbB2 TM domain show that it may undergo dimerization via either one of the two motifs, thus supporting this hypothesis (Fleishman et al. 2002). These findings lead to propose a molecular-switch model for the activation of the receptor in which rotation movements and sliding of each monomer with respect to the other would allow switching between the two dimerization modes, corresponding to active and inactive states.

A similar model could be applied to the two receptors ErbB1 and ErbB2 to explain the process of homo and

heterodimerization. Recent studies have shown that the N-terminal motif of the TM domain does not play a uniform role in the dimerization process: the N-terminal motif of the ErbB2 TM domain appears to be involved in homodimerization, but that of ErbB1 is not sufficient for the formation of homodimers (Gerber et al. 2004). The two distinct recognition motifs of the TM domain of ErbB1 are supposed to be specific for different interactions, the N-terminal motif being necessary for heterodimerization with ErbB2 while the C-terminal motif is needed for homodimerization. The TM domain with two distinct recognition motifs may drive two distinct functions.

It has been suggested that this molecular-switch model could be a common mechanism of all heterotypic heterodimers (Fleishman et al. 2002). Our results support this hypothesis. The representation of the dimer interface for the two modes of association described for the $HER^{2-3}{}_{TM}$ heterodimer illustrates the possibility of such a mechanism (Fig. 4). When the two segments associate via the N-terminus, the small residues Ser653, Ala657, Gly660 on $HER^{2}{}_{TM}$ and Thr647 and Ala650 on $HER^{3}{}_{TM}$ are completely or partially buried within the interface, while the Gly residues of the second motif on $HER^{2}{}_{TM}$ and one of the two Gly residues on $HER^{3}{}_{TM}$ are fully accessible. On the contrary, when the association occurs via the C-terminus, the four Gly residues, 668 and 672 on $HER^{2}{}_{TM}$ and 660 and 661 on $HER^{3}{}_{TM}$, are completely buried (accessible surface null), while all the small residues of the N-terminus are fully accessible except Ala645 on $HER^{3}{}_{TM}$. The same features are observed for the $HER^{2-1}{}_{TM}$, $HER^{2-4}{}_{TM}$ and $HER^{1-4}{}_{TM}$ heterodimers. For example, in the case of $HER^{2-1}{}_{TM}$, Ser653, Ser656 and Gly660 on $HER^{2}{}_{TM}$ and Thr648 and Gly652 on $HER^{1}{}_{TM}$ are buried at the interface in the case of the N-terminal association, while Gly and Ala of the GxxxG motif at the C-terminus of the two monomers are fully exposed. These same Gly residues (672 on $HER^{2}{}_{TM}$ and 665 on $HER^{1}{}_{TM}$) are oriented towards the interface and totally inaccessible, while almost all the small residues at the N-terminus are fully accessible when the association is mediated via the C-terminus. The correlation between accessible residues at the C-terminus and buried residues at the N-terminus, and reciprocally, is less pronounced for $HER^{3-4}{}_{TM}$ and $HER^{1-3}{}_{TM}$ probably because of helix deformations.

Our TM heterodimer models demonstrate that the two dimerization modes are associated to distinct helix orientation resulting in different sites for intermolecular interactions. It is reasonable to suggest that these two modes of association could be used by the ErbB2 receptor supposed to mediate lateral information transfer between the other receptors (Shankaran et al. 2006). Further analyses of the MD models in explicit membrane environment could help in understanding such mechanisms.

Hierarchy of interactions

Studies undertaken on the whole receptors indicate that inter ErbB receptor cross talks obey a hierarchy almost similar to that observed for the TM domains (Table 5). According to Tzahar et al. (1996), ErbB2 receptor interacts with the three other members, with the most potent interaction being with ErbB3. The superior ability for ErbB2 to form dimers with ErbB1 and ErbB3 is also described for the TM domains. Heterodimerization of ErbB3 and ErbB4 receptors was not detected using affinity labeling and co-immuno precipitation experiments (Tzahar et al. 1996), but interactions exist as demonstrated by Riese et al. (1995). Apparent discrepancies are explained by the differences in ErbB expression levels and cellular environments. Otherwise, studies based on a detailed kinetic model on receptors subjected to ligand stimulation have shown that ErbB3–ErbB2 heterodimers are more abundant than ErbB2–ErbB1 species, which are more abundant than the heterodimers formed by ErbB1 and ErbB3 (Shankaran et al. 2006). Heterodimerization of the ErbB4 receptor was not reported in this last study.

Some discrepancies exist between experimental data on the whole receptors and the TM domains. Experiments on the whole receptors take into account the environment of the cell and the presence of other receptors and their ligands. Experiments on the TM domains ignore the effects of the extra and intracellular domains. In addition, TM domain experiments used synthesized peptides reconstituted in micelles and sequences contained minor changes in order to enhance FRET signals.

A scale of affinity of the TM domains can be proposed by analyzing energy terms. We keep in mind that theoretical data reflect exclusively the intrinsic properties of the exact sequence of TM domains and that other energy contributions, in particular those induced by the membrane effects, must be taken into account to quantify more precisely helix–helix binding affinities (Lomize et al. 2004). The membrane effects are discussed below.

As shown in Table 5, the scale of affinity deduced from helix–helix interactions slightly differs from that deduced from $\Delta G^{\circ}{}_{bind}$ values. The strength of helix–helix interactions places $HER^{2-1}{}_{TM}$ and $HER^{1-3}{}_{TM}$ at the two first ranks of the hierarchy. Interestingly, these two types of association occupy, respectively, the first and the third rank of the experimental hierarchy (Duneau et al. 2007). According to the binding free energy values, the order is slightly modified. $HER^{1-3}{}_{TM}$ is shifted to the first rank while $HER^{2-1}{}_{TM}$ is shifted to the fourth rank. The most striking divergence between experimental and theoretical hierarchy is observed for the pair $HER^{3}{}_{TM}$–$HER^{4}{}_{TM}$. Helix–helix interactions are generally stronger than that observed for the other dimer types and can be explained by

the side chain backbone hydrogen bonds formed at the N-terminal extremity of the two monomers involving Thr643 of $HER^{3}{}_{TM}$. These two TM segments exhibit the greatest number of aromatic residues among the other TM pairs leading to a large increase of van der Waals interactions. For example, for the two representative models described in Table 4, the Phe and Tyr side chains are stacked at the C-termination, and these aromatic residues can provide specificity in TM assembly (Sal-Man et al. 2007).

Calculations in implicit membrane have been performed to evaluate the solvation free energy term (EEF1 module included in CHARMM; Lazaridis 2003). The scale of affinity is very similar to that obtained from helix–helix interaction analyses.

Clearly, our theoretical models are unable to represent the full complexity of the interplay of the different receptors where various factors like the structure of the extracellular and intracellular domain, ligand preference and environment play a role.

Membrane environment effects

Helix–helix association is controlled by a delicate balance of forces, depending on the precise composition of the TM segments and on the properties of the membrane environment. The width of the lipid bilayers has the most pronounced effects on membrane protein tertiary structure. Tilting, helix rotation angle that both reflect the intrinsic properties of the TM segments and also helix flexing are the responses to bilayer mismatch (Nyholm et al. 2007; Yeagle et al. 2007). However, when helix–helix recognition motifs are present in the TM segments, association can be highly specific, and helix–helix interactions are the driving forces for the association.

These membrane effects have been observed in the case of the GpA_{TM} dimer. Simulations performed in DPC (dodecyl phosphocholine) micelles and DMPC (dimytistoyl phosphatidylcholine) bilayers (Cuthbertson et al. 2006) converge to a common model close to the NMR structure (MacKenzie et al. 1997). The same observations have been made by examining the GpA_{TM} dimer behavior in different fluid phase bilayers (Petrache et al. 2000). It is found that the membrane environment modulates the subspace of structurally accessible states of the dimer depending on the length of the lipid chains and the acyl chain saturation. Motions and atomic fluctuations are modulated by contacting lipids, but the average structure is not changed.

One may reasonably think that similar membrane effects would be observed in the case of the $HER^{i-j}{}_{TM}$ heterodimers. We have shown the specificity of interactions between the HER_{TM} segments involving GxxxG sequence motifs, and one may expect that the structural models proposed from simulations in vacuo will not be significantly changed in the membrane environment. However, the membrane environment may change the scale of affinity. In particular, the aromatic residues localized at the lipid–water interface may affect the association propensity, particularly for the $HER^{3}{}_{TM}$ and $HER^{4}{}_{TM}$ pair [(Johnson et al. 2007): Sal-Man 2007 #1876].

Other parts of the receptor are involved in dimerization

Dimerization is driven entirely by receptor–receptor interactions. X-ray crystal structures of the ErbB extracellular regions in different activation states provided significant insight into receptor dimerization and activation (Burgess et al. 2003; Dawson et al. 2007 and references therein; Riese et al. 2007). A critical dimerization arm in the cysteine-rich domain II of the extracellular domain provides the majority of contacts across the interface (Garrett et al. 2002; Ogiso et al. 2002). Although it is a major contribution to the association process, it is not sufficient and additional contacts, induced by large domain rearrangement promoted by growth factor binding, are necessary to stabilize receptor dimerization. Smaller interaction sites are also made by other parts of domain II and IV of the extracellular domain (Dawson et al. 2005).

Table 5 Hierarchy of interactions of the ErbB receptors defined from experiments for the whole ErbB receptors (a) (Tzahar et al. 1996) and for the TM domains (b) (Duneau et al. 2007)

Affinity scale	Rank	1	>2	>3	>4	>5	>6
Whole receptor (a)	Experiments	ErbB2-3	ErbB2-1	ErbB2-4	ErbB1-3	ErbB1-4	–
Whole receptor (c)	Kinetic model	ErbB2-3	ErbB2-1	ErbB1-3	–	–	–
TM domain (b)	Experiments	HER^{2-1}	HER^{2-3}	HER^{1-3}	HER^{2-4}	HER^{1-4}	HER^{3-4}
TM domain (this work)	(d)	HER^{2-1}	HER^{1-3}	HER^{3-4}	HER^{2-3}	HER^{2-4}	HER^{1-4}
	(e)	HER^{1-3}	HER^{3-4}	HER^{2-3}	HER^{2-1}	HER^{2-4}	HER^{1-4}
	(f)	HER^{1-3}	HER^{2-1}	HER^{3-4}	HER^{2-3}	HER^{1-4}	HER^{2-4}

Data from Shankaran et al. (c) (2006) are available only for the three receptors ErbB1, 2 and 3. A theoretical hierarchy is proposed from the best representative structures (see Table 4) based on the magnitude of helix–helix interactions (d) and ΔG bind values (e). (f) Affinity scale deduced from calculations in implicit membrane model (Brooks et al. 1983; Lazaridis 2003)

In addition, the different ErbB ligands could induce different configurations of domain II in the extracellular domain and thus modify receptor–receptor contacts.

Intermolecular interactions between intracellular regions are also revealed by X-ray structures of the kinase domain of the EGF receptor. Analysis of the crystal lattice shows two potentially important dimers (Landau et al. 2004; Zhang et al. 2006). One is symmetric with the two domains interacting in a head-to-tail fashion and the second one is an asymmetric dimer in which the C-lobe of one kinase domain juxtaposes against the N-lobe of the second kinase domain. The symmetric dimer is not involved in the activation process, but the asymmetric dimer stabilizes the kinase domain of one of the receptor monomers in the active conformation.

A general model for dimerization and activation of all the members in the family has been proposed from X-ray structures of extra- and intracellular domains of ErbB receptors (Zhang et al. 2006). This model, although supported by abundant experimental data, cannot give a complete description of all interaction sites. ErbB receptors are controlled by a dozen growth factors that could alter the structure of the whole receptors inducing changes in homo- and/or heterodimerization process.

The question of the relative contribution of the extracellular domain and the TM domain to dimerization process in the absence of ligand is yet to be answered. Both domains contribute to receptor–receptor interactions, and also the catalytic domain, but their relative contributions are unknown (Li and Hristova 2006; Tanner and Kyte 1999). Attempts have been made to build 3D dimer models of the truncated EGF receptor (Duneau et al. 2006) and the full-length ErbB2 receptor (Bagossi et al. 2005), but they cannot give an account of the complexity of the interactions between the full receptors and thus a quantitative evaluation of the strength of interaction between each domain is out of reach.

Conclusion

Dimerization of the ErbB receptor family is governed by complex interactions that involve multiple parts of the receptor. Interactions between the extracellular domains of the receptors are not sufficient to stabilize dimers and additional interactions in the TM spans may aid in their stabilization.

The present study allows a better understanding of the nature of the interactions within heterodimers. The prediction of TM heterodimerization models leads to the description of two modes of association and the explicit identification of dimer interfaces. The two modes of association, mediated either by one of the two dimerization motifs of the TM domain, and associated with distinct orientation of the helices could play a major role in competition processes between the receptors.

To our knowledge, this is the first study devoted to the prediction of models of transmembrane heterodimerization of the ErbB receptors. MD models add to the understanding of the complex interaction network of the ErbB receptors and can serve to design new experiments.

References

Adamian L, Liang J (2001) Helix–helix packing and interfacial pairwise interactions of residues in membrane proteins. J Mol Biol 311:891–907

Aifa S, Aydin J, Nordvall G, Lundstrom I, Svensson SP, Hermanson O (2005) A basic peptide within the juxtamembrane region is required for EGF receptor dimerization. Exp Cell Res 302:108–114

Aifa S, Miled N, Frikha F, Aniba MR, Svensson SP, Rebai A (2006) Electrostatic interactions of peptides flanking the tyrosine kinase domain in the epidermal growth factor receptor provides a model for intracellular dimerization and autophosphorylation. Proteins 62:1036–1043

Bagossi P, Horvath G, Vereb G, Szollosi J, Tozser J (2005) Molecular modeling of nearly full-length ErbB2 receptor. Biophys J 88:1354–1363

Bargmann CI, Hung MC, Weinberg RA (1986) The neu oncogene encodes an epidermal growth factor receptor-related protein. Nature 319:226–230

Bargmann CI, Weinberg RA (1988a) Increased tyrosine kinase activity associated with the protein encoded by the activated neu oncogene. Proc Natl Acad Sci USA 85:5394–5398

Bargmann CI, Weinberg RA (1988b) Oncogenic activation of the neu-encoded receptor protein by point mutation and deletion. EMBO J 7:2043–2052

Bell CA, Tynan JA, Hart KC, Meyer AN, Robertson SC, Donoghue DJ (2000) Rotational coupling of the transmembrane and kinase domains of the Neu receptor tyrosine kinase. Mol Biol Cell 11:3589–3599

Bouyain S, Longo PA, Li S, Ferguson KM, Leahy DJ (2005) The extracellular region of ErbB4 adopts a tethered conformation in the absence of ligand. Proc Natl Acad Sci USA 102:15024–15029

Bowie JU (1997) Helix packing in membrane proteins. J Mol Biol 272:780–789

Brooks BR, Bruccoleri RE, Olafson BD, States DJ, Swaminathan S, Karplus M (1983) CHARMM: a program for macromolecular energy minimization, and dynamics calculations. J Comp Chem 4:187–217

Burgess AW, Cho HS, Eigenbrot C, Ferguson KM, Garrett TP, Leahy DJ, Lemmon MA, Sliwkowski MX, Ward CW, Yokoyama S (2003) An open-and-shut case? Recent insights into the activation of EGF/ErbB receptors. Mol Cell 12:541–552

Cho HS, Leahy DJ (2002) Structure of the extracellular region of HER3 reveals an interdomain tether. Science 297:1330–1333

Chothia C, Levitt M, Richardson D (1981) Helix to helix packing in proteins. J Mol Biol 145:215–250

Citri A, Yarden Y (2006) EGF-ERBB signalling: towards the systems level. Nat Rev Mol Cell Biol 7:505–516

Coussens L, Yang-Feng TL, Liao YC, Chen E, Gray A, McGrath J, Seeburg PH, Libermann TA, Schlessinger J, Francke U et al (1985) Tyrosine kinase receptor with extensive homology to

EGF receptor shares chromosomal location with neu oncogene. Science 230:1132–1139
Cuthbertson JM, Bond PJ, Sansom MS (2006) Transmembrane helix–helix interactions: comparative simulations of the glycophorin a dimer. Biochemistry 45:14298–14310
Dawson JP, Weinger JS, Engelman DM (2002) Motifs of serine and threonine can drive association of transmembrane helices. J Mol Biol 316:799–805
Dawson JP, Melnyk RA, Deber CM, Engelman DM (2003) Sequence context strongly modulates association of polar residues in transmembrane helices. J Mol Biol 331:255–262
Dawson JP, Berger MB, Lin CC, Schlessinger J, Lemmon MA, Ferguson KM (2005) Epidermal growth factor receptor dimerization and activation require ligand-induced conformational changes in the dimer interface. Mol Cell Biol 25:7734–7742
Dawson JP, Bu Z, Lemmon MA (2007) Ligand-induced structural transitions in ErbB receptor extracellular domains. Structure 15:942–954
Di Fiore PP, Pierce JH, Kraus MH, Segatto O, King CR, Aaronson SA (1987) erbB-2 is a potent oncogene when overexpressed in NIH/3T3 cells. Science 237:178–182
Duneau JP, Vegh AP, Sturgis JN (2006) Transmembrane domains arbitrate HER receptor family dimerization
Duneau JP, Vegh AP, Sturgis JN (2007) A dimerization hierarchy in the transmembrane domains of the HER receptor family. Biochemistry 46:2010–2019
Eilers M, Shekar SC, Shieh T, Smith SO, Fleming PJ (2000) Internal packing of helical membrane proteins. Proc Natl Acad Sci USA 97:5796–5801
Ferguson KM, Berger MB, Mendrola JM, Cho HS, Leahy DJ, Lemmon MA (2003) EGF activates its receptor by removing interactions that autoinhibit ectodomain dimerization. Mol Cell 11:507–517
Eilers M, Patel AB, Liu W, Smith SO (2002) Comparison of helix interactions in membrane and soluble alpha-bundle proteins. Biophys J 82:2720–2736
Fleishman SJ, Schlessinger J, Ben-Tal N (2002) A putative molecular-activation switch in the transmembrane domain of erbB2. Proc Natl Acad Sci USA 99:15937–15940
Garrett TP, McKern NM, Lou M, Elleman TC, Adams TE, Lovrecz GO, Zhu HJ, Walker F, Frenkel MJ, Hoyne PA, Jorissen RN, Nice EC, Burgess AW, Ward CW (2002) Crystal structure of a truncated epidermal growth factor receptor extracellular domain bound to transforming growth factor alpha. Cell 110:763–773
Garrett TP, McKern NM, Lou M, Elleman TC, Adams TE, Lovrecz GO, Kofler M, Jorissen RN, Nice EC, Burgess AW, Ward CW (2003) The crystal structure of a truncated ErbB2 ectodomain reveals an active conformation, poised to interact with other ErbB receptors. Mol Cell 11:495–505
Gerber D, Sal-Man N, Shai Y (2004) Two motifs within a transmembrane domain, one for homodimerization and the other for heterodimerization. J Biol Chem 279:21177–21182
Gratkowski H, Lear JD, DeGrado WF (2001) Polar side chains drive the association of model transmembrane peptides. Proc Natl Acad Sci USA 98:880–885
Gullick WJ (2001) The Type 1 growth factor receptors and their ligands considered as a complex system. Endocr Relat Cancer 8:75–82
Javadpour MM, Eilers M, Groesbeek M, Smith SO (1999) Helix packing in polytopic membrane proteins: role of glycine in transmembrane helix association. Biophys J 77:1609–1618
Johnson RM, Hecht K, Deber CM (2007) Aromatic and cation-pi interactions enhance helix–helix association in a membrane environment. Biochemistry 46:9208–9214
Karunagaran D, Tzahar E, Beerli RR, Chen X, Graus-Porta D, Ratzkin BJ, Seger R, Hynes NE, Yarden Y (1996) ErbB-2 is a common auxiliary subunit of NDF and EGF receptors: implications for breast cancer. Embo J 15:254–264
Killian JA, von Heijne G (2000) How proteins adapt to a membrane–water interface. Trends Biochem Sci 25:429–434
Kleiger G, Grothe R, Mallick P, Eisenberg D (2002) GXXXG and AXXXA: common alpha-helical interaction motifs in proteins, particularly in extremophiles. Biochemistry 41:5990–5997
Kraus MH, Issing W, Miki T, Popescu NC, Aaronson SA (1989) Isolation and characterization of ERBB3, a third member of the ERBB/epidermal growth factor receptor family: evidence for overexpression in a subset of human mammary tumors. Proc Natl Acad Sci USA 86:9193–9197
Landau M, Fleishman SJ, Ben-Tal N (2004) A putative mechanism for downregulation of the catalytic activity of the EGF receptor via direct contact between its kinase and C-terminal domains. Structure 12:2265–2275
Lazaridis T (2003) Effective energy function for proteins in lipid membranes. Proteins 52:176–192
Lemmon MA, Bu Z, Ladbury JE, Zhou M, Pinchasi D, Lax I, Engelman DM, Schlessinger J (1997) Two EGF molecules contribute additively to stabilization of the EGFR dimer. EMBO J 16:281–294
Li E, Hristova K (2006) Role of receptor tyrosine kinase transmembrane domains in cell signaling and human pathologies. Biochemistry 45:6241–6251
Linggi B, Carpenter G (2006) ErbB receptors: new insights on mechanisms and biology. Trends Cell Biol 16:649–656
Lomize AL, Pogozheva ID, Mosberg HI (2004) Quantification of helix–helix binding affinities in micelles and lipid bilayers. Protein Sci 13:2600–2612
MacKenzie KR, Prestegard JH, Engelman DM (1997) A transmembrane helix dimer: structure and implications. Science 276:131–133
MacKerell AD Jr, Brooks B, Brooks CL III, Nilsson L, Roux B, Won Y, Karplus M (1998) CHARMM: the energy function and its parameterization with an overview of the program, P v R, vol 1. In: Schleyer et al. (eds) The encyclopedia of computational chemistry. Wiley, Chichester, pp 271–277
Mattoon D, Klein P, Lemmon MA, Lax I, Schlessinger J (2004) The tethered configuration of the EGF receptor extracellular domain exerts only a limited control of receptor function. Proc Natl Acad Sci USA 101:923–928
Mendrola JM, Berger MB, King MC, Lemmon MA (2002) The single transmembrane domains of ErbB receptors self-associate in cell membranes. J Biol Chem 277:4704–4712
Moriki T, Maruyama H, Maruyama IN (2001) Activation of preformed EGF receptor dimers by ligand-induced rotation of the transmembrane domain. J Mol Biol 311:1011–1026
Nyholm TK, Ozdirekcan S, Killian JA (2007) How protein transmembrane segments sense the lipid environment. Biochemistry 46:1457–1465
Ogiso H, Ishitani R, Nureki O, Fukai S, Yamanaka M, Kim JH, Saito K, Sakamoto A, Inoue M, Shirouzu M, Yokoyama S (2002) Crystal structure of the complex of human epidermal growth factor and receptor extracellular domains. Cell 110:775–787
Olayioye MA, Neve RM, Lane HA, Hynes NE (2000) The ErbB signaling network: receptor heterodimerization in development and cancer. EMBO J 19:3159–3167
Petrache HI, Grossfield A, MacKenzie KR, Engelman DM, Woolf TB (2000) Modulation of Glycophorin A transmembrane helix interactions by lipid bilayers: molecular dynamics calculations. J Mol Biol 302:727–746
Plowman GD, Culouscou JM, Whitney GS, Green JM, Carlton GW, Foy L, Neubauer MG, Shoyab M (1993) Ligand-specific activation of HER4/p180erbB4, a fourth member of the epidermal growth factor receptor family. Proc Natl Acad Sci USA 90:1746–1750

Prigent SA, Lemoine NR (1992) The type 1 (EGFR-related) family of growth factor receptors and their ligands. Prog Growth Factor Res 4:1–24

Prigent SA, Gullick WJ (1994) Identification of c-erbB-3 binding sites for phosphatidylinositol 3'-kinase and SHC using an EGF receptor/c-erbB-3 chimera. Embo J 13:2831–41

Riese DJ, van Raaij TM, Plowman GD, Andrews GC, Stern DF (1995) The cellular response to neuregulins is governed by complex interactions of the erbB receptor family. Mol Cell Biol 15:5770–5776 Published erratum appears in Mol Cell Biol 1996 Feb;16(2):735

Riese DJ 2nd, Gallo RM, Settleman J (2007) Mutational activation of ErbB family receptor tyrosine kinases: insights into mechanisms of signal transduction and tumorigenesis. Bioessays 29:558–565

Sako Y, Minoghchi S, Yanagida T (2000) Single-molecule imaging of EGFR signalling on the surface of living cells. Nat Cell Biol 2:168–172

Sal-Man N, Gerber D, Bloch I, Shai Y (2007) Specificity in transmembrane helix–helix interactions mediated by aromatic residues. J Biol Chem 282:19753–19761

Salomon DS, Brandt R, Ciardiello F, Normanno N (1995) Epidermal growth factor-related peptides and their receptors in human malignancies. Crit Rev Oncol Hematol 19:183–232

Samna Soumana O, Garnier N, Genest M (2007) Molecular dynamics simulation approach for the prediction of transmembrane helix–helix heterodimers assembly. Eur Biophys J 36:1071–10782

Schlessinger J (2000) Cell signaling by receptor tyrosine kinases. Cell 103:211–225

Senes A, Gerstein M, Engelman DM (2000) Statistical analysis of amino acid patterns in transmembrane helices: the GXXXG motif occurs frequently and in association with beta-branched residues at neighboring positions. J Mol Biol 296:921–936

Shankaran H, Wiley HS, Resat H (2006) Modeling the effects of HER/ErbB1-3 coexpression on receptor dimerization and biological response. Biophys J 90:3993–4009

Stanley AM, Fleming KG (2005) The transmembrane domains of ErbB receptors do not dimerize strongly in micelles. J Mol Biol 347:759–772

Sternberg MJ, Gullick WJ (1990) A sequence motif in the transmembrane region of growth factor receptors with tyrosine kinase activity mediates dimerization. Protein Eng 3:245–248

Tanner KG, Kyte J (1999) Dimerization of the extracellular domain of the receptor for epidermal growth factor containing the membrane-spanning segment in response to treatment with epidermal growth factor. J Biol Chem 274:35985–35990

Tzahar E, Waterman H, Chen X, Levkowitz G, Karunagaran D, Lavi S, Ratzkin BJ, Yarden Y (1996) A hierarchical network of interreceptor interactions determines signal transduction by Neu differentiation factor/neuregulin and epidermal growth factor. Mol Cell Biol 16:5276–5287

Tzahar E, Pinkas-Kramarski R, Moyer JD, Klapper LN, Alroy I, Levkowitz G, Shelly M, Henis S, Eisenstein M, Ratzkin BJ, Sela M, Andrews GC, Yarden Y (1997) Bivalence of EGF-like ligands drives the ErbB signaling network. EMBO J 16:4938–4950

Ullrich A, Coussens L, Hayflick JS, Dull TJ, Gray A, Tam AW, Lee J, Yarden Y, Libermann TA, Schlessinger J, et al (1984) Human epidermal growth factor receptor cDNA sequence and aberrant expression of the amplified gene in A431 epidermoid carcinoma cells. Nature 309:418–425

Walters RF, DeGrado WF (2006) Helix-packing motifs in membrane proteins. Proc Natl Acad Sci USA 103:13658–13663

Warren CM, Landgraf R (2006) Signaling through ERBB receptors: multiple layers of diversity and control. Cell Signal 18:923–933

Weiss TM, van der Wel PC, Killian JA, Koeppe RE 2nd, Huang HW (2003) Hydrophobic mismatch between helices and lipid bilayers. Biophys J 84:379–385

Yamamoto T, Ikawa S, Akiyama T, Semba K, Nomura N, Miyajima N, Saito T, Toyoshima K (1986) Similarity of protein encoded by the human c-erb-B-2 gene to epidermal growth factor receptor. Nature 319:230–234

Yarden Y, Sliwkowski MX (2001) Untangling the ErbB signalling network. Nat Rev Mol Cell Biol 2:127–137

Yeagle PL, Bennett M, Lemaitre V, Watts A (2007) Transmembrane helices of membrane proteins may flex to satisfy hydrophobic mismatch. Biochim Biophys Acta 1768:530–537

Zhang X, Gureasko J, Shen K, Cole PA, Kuriyan J (2006) An allosteric mechanism for activation of the kinase domain of epidermal growth factor receptor. Cell 125:1137–1149

Zhou FX, Merianos HJ, Brunger AT, Engelman DM (2001) Polar residues drive association of polyleucine transmembrane helices. Proc Natl Acad Sci USA 98:2250–2255

Zoete V, Meuwly M, Karplus M (2005) Study of the insulin dimerization: binding free energy calculations and per-residue free energy decomposition. Proteins 61:79–93